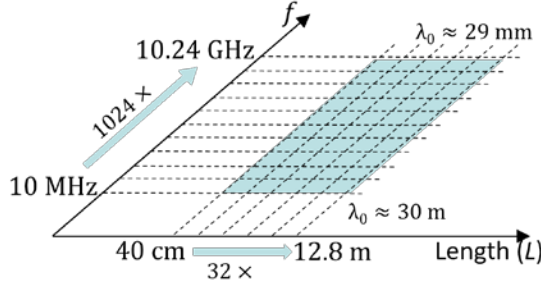


Description of Scattering Object

A perfect electrically conducting (PEC) hexagonal prism.

Length Scale and Frequency Range



The problems of interest cover a range of 32x in physical length scale and 1024x in frequency; the ranges are logarithmically sampled to yield 66 scattering problems. Because the camera boxes are PEC, there are only 16+1 unique scattering problems in Problem Set IIISA. In these problems, the model sizes are in the range $0.013 \leq L/\lambda_0 \leq 438$, where λ_0 is the free-space wavelength.

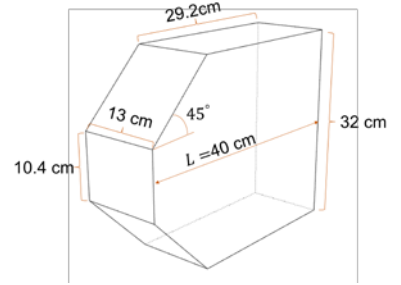
Interesting Features

1. The camera box is designed as a host structure to enable reproducible RCS measurements of ducts. The flat-plate geometrical features of the housing promote strong backscattering in certain directions that are minimally affected by the scattering characteristics of any voids in the box [1].

2. The diagram above shows the smallest camera box in the problem set. The sampling of the frequency range is distorted for this problem:

Scattering from the smallest camera box at frequencies $f \in \{10, 20, 40, 80, 160, 320, 640, 1280, 2560, 5120, 7000, 10240\}$ MHz are included in the problem set. This distortion is because of publicly available measurement data [1] and adds 1 unique scattering problem to the set.

3. The other 5 camera boxes in the problem set IIISA are obtained by scaling all dimensions of the geometry proportionally.



Quantities of Interest

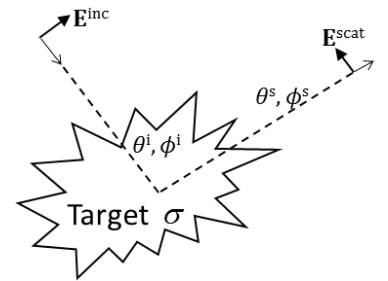
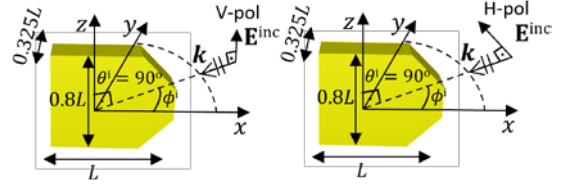
Radar cross section (RCS) definition

$$\sigma_{vu}(\theta^s, \phi^s, \theta^i, \phi^i) = \lim_{R \rightarrow \infty} 4\pi R^2 \frac{|\hat{v}(\theta^s, \phi^s) \cdot \mathbf{E}^{\text{scat}}(\theta^s, \phi^s)|^2}{|\hat{u}(\theta^i, \phi^i) \cdot \mathbf{E}^{\text{inc}}(\theta^i, \phi^i)|^2} : \text{RCS (m}^2\text{)}$$

$$\sigma_{vu,\text{dB}}(\theta^s, \phi^s, \theta^i, \phi^i) = 10 \log_{10} \sigma_{vu} : \text{RCS in dB (dBsm)}$$

$$\sigma_{vu,\text{dB}}^{\text{TH}}(\theta^s, \phi^s, \theta^i, \phi^i) = \max(\sigma_{vu,\text{dB}}, TH_{vu,\text{dB}}) - TH_{vu,\text{dB}} : \text{Thresholded RCS}$$

1. Set $\theta^i = 90^\circ$. Vary $0^\circ \leq \phi^i \leq 180^\circ$ (every 0.5° in the interval).
2. Compute back-scattered $\sigma_{\theta\theta,\text{dB}}$ and $\sigma_{\phi\phi,\text{dB}}$ (the VV- and HH-RCS in dB) at $N_\phi = 361$ scattering directions.



Performance Measures

Error Measure: Simulation errors shall be quantified using

$$\text{avg. err}_{uu,\text{dB}}^{\text{TH}} = \frac{1}{2\pi} \int_0^{2\pi} |\sigma_{uu,\text{dB}}^{\text{TH}}(\phi^s) - \sigma_{uu,\text{dB}}^{\text{ref},\text{TH}}(\phi^s)| d\phi^s \approx \frac{1}{N_\phi} \sum_{n=1}^{N_\phi} |\sigma_{uu,\text{dB}}^{\text{TH}}(\phi^s) - \sigma_{uu,\text{dB}}^{\text{ref},\text{TH}}(\phi^s)| \text{ (dB) for } u \in \{\theta, \phi\}$$

where

$$TH_{uu,\text{dB}} = \max_{\phi^s} \sigma_{uu,\text{dB}}^{\text{ref}} - 80 \text{ (dB)}$$

This error measure discounts errors in RCS values below TH .

Cost Measure: Simulation costs shall be quantified using observed wall-clock time and peak memory/core

$$t_{\text{main}}^{\text{wall}} \text{ (s) and } mem_{\text{main}}^{\text{maxcore}} \text{ (bytes)}$$

as well as the “serialized” CPU time and total memory requirement

$$t_{\text{main}}^{\text{total}} = N_{\text{proc}} \times t_{\text{main}}^{\text{wall}} \text{ (s) and } mem_{\text{main}}^{\text{max}} = N_{\text{proc}} \times mem_{\text{main}}^{\text{maxcore}} \text{ (bytes)}$$

Here, N_{proc} denotes the number of processes used in a parallel simulation. It is expected that results will be reported for at least 2 runs: “Efficient” (small N_{proc}) and “Fast” (large N_{proc}).

Study 1: Error vs. Cost Sweep

Fix frequency and fix camera box dimensions. Simulate many error levels (proxy: mesh densities) for 4 cases:

Case 1: $f=10$ MHz, $L=40$ cm

Case 2: $f=7$ GHz, $L=40$ cm

Case 3: $f=10$ MHz, $L=6.4$ m

Case 4: $f=320$ MHz, $L=6.4$ m

It’s recommended to simulate as many error levels (mesh densities) as possible. 3-5 error levels is typical. A typical error-vs.-cost study will consist of $4 \times 3 = 12$ -20 simulations.

Study 2: Frequency Sweep

Fix camera box dimensions and error level (proxy: mesh density). Simulate many frequencies for 4 cases:

Case 1: $L=40$ cm, error level 1 (coarsest mesh)

Case 2: $L=6.4$ m, error level 1 (coarsest mesh)

Case 3: $L=40$ cm, error level 2 (finer mesh)

Case 4: $L=6.4$ m, error level 2 (finer mesh)

Frequencies shall be chosen as $f \in \{10, 20, 40, \dots, 5120, 10240\}$ MHz. It’s recommended to simulate as many frequencies as possible. A full frequency-sweep study will consist of $4 \times 11 = 44$ simulations.

Study 3: Size Sweep

Fix frequency and error level (proxy: mesh density). Simulate many sizes for 4 cases:

Case 1: $f=10$ MHz, error level 1 (coarsest mesh)

Case 2: $f=320$ MHz, error level 1 (coarsest mesh)

Case 3: $f=10$ MHz, error level 2 (finer mesh)

Case 4: $f=320$ MHz, error level 2 (finer mesh)

Dimensions shall be chosen as $L \in \{40, 80, 120, \dots, 640, 1280\}$ cm. It’s recommended to simulate as many sizes as possible. A full size-sweep study will consist of $4 \times 7 = 28$ simulations.

Reference Quantities of Interest

The following RCS data are made available in the benchmark to enable participants to calibrate their simulators:

8 RCS measurement results corresponding to the smallest camera box ($L=40$ cm) at frequencies $f \in \{2560, 5120, 7000, 10240\}$ MHz. These data are provided for ϕ^i sampled every 0.5° . Note that the high return at $\phi^i = 90^\circ$ saturated the instrumentation radar at 10240 MHz; thus, the measured RCS values near that look angle are inaccurate. The same phenomenon can be observed in Fig. 3 in [1].

4 RCS simulation results for the smallest camera box at the above 4 frequencies found by using the ARCHIE-AIM code, a frequency-domain FFT-accelerated integral-equation solver developed at UT Austin [2]-[4].

References

- [1] A. E. Yilmaz, E. Smith, S. Cox, B. MacKie-Mason, C. C. Courtney, and G. Burchuk, "Camera boxes: a set of complex scattering problems to test EM simulations and measurements," in *Proc. IEEE Antennas Propag. Soc. Int. Symp.*, July 2022.
- [2] M. F. Wu, G. Kaur, and A. E. Yilmaz, "A multiple-grid adaptive integral method for multi-region problems," *IEEE Trans. Antennas Propag.*, vol. 58, no. 5, pp. 1601-1613, May 2010.
- [3] F. Wei and A. E. Yilmaz, "A more scalable and efficient parallelization of the adaptive integral method part I: algorithm," *IEEE Trans. Antennas Propag.*, vol. 62, no.2, pp. 714-726, Feb. 2014.
- [4] J. W. Massey, V. Subramanian, C. Liu, and A. E. Yilmaz, "Analyzing UHF band antennas near humans with a fast integral-equation method," in *Proc. EUCAP*, Apr. 2016.